Image Cover Sheet

CLASSIFICATION	SYSTEM NUMBER
UNCLASSIFIED	501385

TITLE

ON THE FALSE ALARM PROBABILITY FOR AN OVERLAPPED FFT PROCESSOR

System Number:

Patron Number:

Requester:

Notes:

DSIS Use only:

Deliver to:

On the False Alarm Probability for an Overlapped FFT Processor

BRIAN H. MARANDA
Defence Research Establishment Atlantic
Canada

A standard processor for detecting narrowband signals in noise applies the fast Fourier transform (FFT) to overlapped data blocks, and then sums the squared magnitudes of the bins from successive FFTs. The overlap of the data blocks causes these bins to be correlated, even when the noise is white. A simple expression is derived for the probability of false alarm when the covariance matrix of the FFT bins is tridiagonal.

Manuscript received March 10, 1995; revised October 3, 1995.

IEEE Log No. T-AES/32/4/08014.

Author's address: Defence Research Establishment Atlantic, P.O. Box 1012, Dartmouth, N.S., Canada B2Y 3Z7.

I. INTRODUCTION

The fast Fourier transform (FFT) has become the standard tool for detecting a narrowband signal in noise. If the narrowband signal is a pure sinusoid, then the coherent integration time can always be increased by increasing the FFT length. In many cases, however, the signal is a narrowband noise process or a sinusoid that exhibits phase instability. For these cases, the input data are segmented into blocks; the FFT is then applied to each block, and corresponding frequency bins from the sequence of FFTs are integrated (summed) noncoherently. Usually the squared magnitudes of the bins are integrated, yielding a quadratic detector. It can be shown that such a processor is close to optimal in several cases of interest [1, 2].

Often in practice the data blocks are overlapped and a weight function is applied before the FFT is taken. The effect of the overlap is to introduce correlation between the bins of successive FFTs, even when the noise is white. This complicates the performance analysis of the overlapped FFT processor. In this paper, an exact formula is derived for the probability of false alarm for the overlapped processor, under the assumption that each FFT bin is correlated only with the bins from the two time-adjacent FFTs; i.e., the covariance matrix for the FFT bins is tridiagonal. This situation occurs, for example, when the noise is white and the overlap of the data blocks does not exceed 50%.

II. OVERLAPPED FFT PROCESSOR

Denote by $x(n)$ a real-valued time series with time index n, where n ranges over the integers. The data stream is segmented into blocks of N points, with an overlap of $N\gamma$ points. Here γ is the fractional overlap, $0 \le \gamma < 1$, and it is assumed that $N\gamma$ is an integer. The data samples for the mth block are given by

$$x_m(n) = x(n + m(1-\gamma)N), \qquad \text{for} \quad 0 \le n \le N-1. \tag{1}$$

The discrete Fourier transform of the mth block is

$$X_m(\omega) = \sum_{n=0}^{N-1} a(n) x_m(n) e^{-i\omega n} \tag{2}$$

where ω is the analysis frequency and $a(n)$ is a weighting function. In practice, the FFT is used to rapidly compute the Fourier coefficients in (2) on a frequency grid with spacing $2\pi/N$, but in the subsequent derivation we consider only a single frequency and will often omit ω from the notation. Let $\mathbf{x}$ denote the column vector formed from the Fourier coefficients $X_m(\omega)$ of M consecutive data blocks:

$$\mathbf{x} = (X_1, X_2, \ldots, X_M)^t$$

where t denotes transpose. The detection statistic is then the quadratic form $q \equiv \mathbf{x}^*\mathbf{x}$, where the asterisk denotes conjugate transpose. Specifically, the detector operates by comparing q to a threshold T: when $q > T$ the bin at frequency ω is assumed to contain a signal, and when $q < T$ the bin is assumed to contain noise alone. (The case $q = T$ occurs with probability zero and can be assigned arbitrarily.)

The detector performance is characterized by the probabilities of detection and false alarm, P_d and P_{fa}. We are concerned here with the latter, defined as the probability that the noise alone will exceed the threshold:

$$P_{fa} = \int_T^\infty f_q(x)\,dx \tag{3}$$

where $f_q(x)$ is the probability density function (pdf) of the detection statistic q when noise only is present. To proceed further, a statistical characterization of the noise is required. It is assumed that when a signal is absent the input time series $x(n)$ is zero-mean Gaussian noise. The Fourier coefficients in (2) are then complex Gaussian random variables, and the probability distribution of the vector $\mathbf{x}$ is determined completely by its second-order statistics. Clearly $E\{\mathbf{x}\} = \mathbf{0}$, and we denote the covariance matrix by $\mathbf{K}_M = E\{\mathbf{x}\mathbf{x}^*\}$. A specific form for the matrix $\mathbf{K}_M$ is considered in the next section. It can also be shown that $E\{\mathbf{x}\mathbf{x}^t\} \cong \mathbf{0}$ except when ω is near the band edges (i.e., within a few binwidths of zero frequency or the foldover frequency). This last condition ensures that $\mathbf{x}$ has a complex Gaussian distribution as defined in [3, 4].

We now introduce the characteristic function of q, defined by $\phi_q(\xi) = E\{\exp(i\xi q)\}$. Since q is a quadratic form in complex Gaussian variables, it follows that [4]

$$\phi_q(\xi) = (\det(\mathbf{I} - i\xi\mathbf{K}_M))^{-1} = \prod_{m=1}^{M}(1 - i\xi\lambda_m)^{-1}$$

where det(·) denotes matrix determinant and the λ_m are the eigenvalues of the covariance matrix $\mathbf{K}_M$. Any covariance matrix is Hermitian and positive semidefinite, and hence the eigenvalues of $\mathbf{K}_M$ are real-valued and satisfy $\lambda_m \geq 0$. It is assumed that the eigenvalues are distinct and that $\lambda_m > 0$; these assumptions hold in the specific case examined in Section III.

The pdf f_q can be obtained by inverting the characteristic function:

$$f_q(x) = \frac{1}{2\pi}\int_{-\infty}^{\infty} \phi_q(\xi)e^{-i\xi x}\,d\xi. \tag{4}$$

For this application, however, it is more convenient to use formulas that yield P_{fa} directly from the characteristic function without finding f_q as an intermediate step. Such formulas can be found, for example, in [5]. Another approach is to substitute (4) into (3) and then interchange the order of integration [6]. However, in order that $e^{-i\xi x} \to 0$ as $x \to \infty$, it is necessary to displace the path of integration below the real axis. Also, the integrand in (4) has poles $z_m \equiv -i/\lambda_m$ located on the lower imaginary axis. We find that

$$P_{fa} = \frac{1}{2\pi i}\int_\Gamma \frac{e^{-iTz}}{z}\phi_q(z)\,dz \tag{5}$$

where $\phi_q(z) = \prod_m (1 - z/z_m)^{-1}$ and the contour Γ is a line below the real axis, but above the poles z_m. Cauchy's Theorem in fact implies that the contour Γ can be taken to be any closed contour enclosing the poles z_m in the clockwise (negative) direction, excluding the pole at $z = 0$. Since the eigenvalues are distinct, the poles are simple and an application of the residue calculus yields the formula

$$P_{fa} = \sum_{m=1}^{M} A_m e^{-T/\lambda_m} \tag{6}$$

where the coefficients A_m are given by

$$A_m = \lambda_m^{M-1}\prod_{\substack{k=1\\k\neq m}}^{M}\frac{1}{\lambda_m - \lambda_k}, \qquad (1 \leq m \leq M). \tag{7}$$

(The coefficients A_m may also be interpreted as coefficients in the partial-fraction decomposition of the characteristic function.) To use formulas (6) and (7), the eigenvalues must be computed. In general this may be done numerically after forming the matrix $\mathbf{K}_M$, although in the next section explicit expressions for the eigenvalues λ_m and the coefficients A_m are obtained for a useful special case.

III. TRIDIAGONAL $\mathbf{K}_M$

So far the development has been of a general nature, with the restriction that the input time series $x(n)$ is a zero-mean Gaussian process. It is now further assumed that 1) the input is white, with $E\{x(m)x(n)\} = \delta_{m,n}\sigma^2$, and 2) the data overlap does not exceed 50%; i.e., $\gamma \leq 0.5$. In this case the matrix $\mathbf{K}_M$ is tridiagonal, since each FFT is correlated only with its two neighbors. It can be shown directly from definitions (1) and (2) that the diagonal entries of $\mathbf{K}_M$ are given by $k_{m,m} = \sigma^2 A^2$, where

$$A^2 = \sum_{n=0}^{N-1} a^2(n).$$

Define $\sigma_0^2 = \sigma^2 A^2$ to be the output variance, so that $k_{m,m} = \sigma_0^2$. It can also be shown that the entries above the main diagonal are given by $k_{m,m+1} = \sigma_0^2 \varrho e^{-i\omega N'}$, where $N' = (1 - \gamma)N$ and ϱ is a correlation coefficient

given by

$$\varrho = \frac{1}{A^2} \sum_{n=0}^{N-N'-1} a(n)a(n+N'). \tag{8}$$

The subdiagonal entries are determined by the Hermitian nature of $\mathbf{K}_M$. When there is no overlap, so that $N' = N$, the sum in (8) is to be interpreted as giving $\varrho = 0$. Since the weights $a(n)$ are always positive in practice, we have in general that $\varrho \geq 0$. Also, because the overlap does not exceed 50% it follows that $N' \geq \frac{1}{2}N$, and this fact in conjunction with an application of the Cauchy–Schwartz inequality to (8) can be used to prove $\varrho \leq \frac{1}{2}$. Hence $0 \leq \varrho \leq \frac{1}{2}$ for the present case.

For ease in the subsequent derivation, it is assumed that $\sigma_0^2 = 1$. As noted in the remarks at the end of this section, this assumption does not entail a loss of generality. Then $\mathbf{K}_M$ is a tridiagonal matrix whose diagonal entries are unity, the entries above and below the main diagonal being $\varrho e^{-i\omega N'}$ and $\varrho e^{i\omega N'}$, respectively. Letting $p_M(\lambda) = \det(\mathbf{K}_M - \lambda \mathbf{I})$ denote the characteristic polynomial of $\mathbf{K}_M$, it can be shown by expanding the determinant about its first column that $p_M(\lambda)$ satisfies the recurrence equation

$$p_M(\lambda) = (1-\lambda)p_{M-1}(\lambda) - \varrho^2 p_{M-2}(\lambda), \qquad (M \geq 2) \tag{9}$$

with $p_0(\lambda) = 1$ and $p_1(\lambda) = 1-\lambda$. Note that the phases $e^{\pm i\omega N'}$ do not appear in (9), and thus have no effect on the eigenvalues. The above recurrence equation can be solved using z-transform techniques [7] to find that $p_M(\lambda)$ has the form

$$p_M(\lambda) = \varrho^M \frac{\sin(M+1)\psi}{\sin\psi} \tag{10}$$

where $\lambda = 1 - 2\varrho\cos\psi$. If desired, $p_M(\lambda)$ can be written explicitly as a polynomial in λ by first expressing $\sin(M+1)\psi/\sin\psi$ in (10) as a polynomial in $\cos\psi$ (see, for example, [8, §1.33]) and then substituting $\cos\psi = (1-\lambda)/2\rho$. However, for analytical work the implicit form (10) is more convenient. In particular, the eigenvalues λ_m of $\mathbf{K}_M$ are just the M zeros of $p_M(\lambda)$, and inspection of (10) immediately yields

$$\lambda_m = 1 - 2\varrho\cos\psi_m$$

where $\psi_m = m\pi/(M+1)$ for $m = 1,\ldots,M$.

A simple formula for the coefficients A_m in (7) can now be obtained from the characteristic polynomial $p_M(\lambda)$. This polynomial can be written in the form

$$p_M(\lambda) = (-1)^M \prod_{m=1}^{M} (\lambda - \lambda_m)$$

where the factor $(-1)^M$ has been determined by examining the recurrence equation (9) for large values of λ. Thus the coefficients A_m can be written in the form

$$A_m = (-1)^M \lambda_m^{M-1} \lim_{\lambda\to\lambda_m} \frac{\lambda - \lambda_m}{p_M(\lambda)} = (-1)^M \frac{\lambda_m^{M-1}}{p_M'(\lambda_m)}$$

where the prime denotes differentiation. Applying the chain rule to (10) now yields

$$p_M'(\lambda) = \varrho^M \frac{d}{d\psi}\left\{\frac{\sin(M+1)\psi}{\sin\psi}\right\}\frac{d\psi}{d\lambda}.$$

Using the fact that $d\psi/d\lambda = (d\lambda/d\psi)^{-1} = (2\varrho\sin\psi)^{-1}$, the previous equation becomes, upon taking the derivative with respect to ψ and substituting $\lambda = \lambda_m$,

$$p_M'(\lambda_m) = (-1)^m \frac{(M+1)\varrho^{M-1}}{2\sin^2\psi_m}.$$

We thus finally arrive at the expression

$$P_{fa} = \frac{2(-1)^M}{(M+1)\varrho^{M-1}} \sum_{m=1}^{M} (-1)^m (\sin\psi_m)^2 \lambda_m^{M-1} e^{-T/\lambda_m} \tag{11}$$

for the probability of false alarm. This formula is the main result of this work. Its suitability for numerical work is examined in Section IV.

This is an appropriate point to make several remarks concerning (11). First, it may appear that the formula gives the incorrect behavior $P_{fa} = O(1/\varrho^{M-1})$ as $\varrho \to 0+$. However, the eigenvalues λ_m also depend on ϱ, and it may be shown from (11) that in fact P_{fa} has a power series expansion of the form

$$P_{fa} = e^{-T}(c_0 + c_2\varrho^2 + c_4\varrho^4 + \cdots) \tag{12}$$

where the coefficients c_k depend on M and T. Explicit expressions for these coefficients can be found from (11), although the algebra is very tedious. The coefficients to fourth order are

$$\begin{aligned} c_0 &= \sum_{m=0}^{M-1} \frac{T^m}{m!} \\ c_2 &= \frac{(M-1)}{(M+1)!} T^M [T - (M+1)] \\ c_4 &= \frac{(M^2+M-4)}{2(M+3)!} T^M \\ &\quad \times [T^3 - 3(M+3)T^2 + 3(M+2)_2 T - (M+1)_3] \end{aligned} \tag{13}$$

where $(a)_k = a(a+1)\cdots(a+k-1)$ is Pochhammer's notation.

A second remark concerns normalization factors. In the above derivation, we set $\sigma_0^2 = 1$. It can be shown

that when $\sigma_0^2 \neq 1$, (11)–(13) remain valid if the symbol T is replaced by T/σ_0^2. Furthermore, if the detection statistic q is normalized by dividing by M, then T should be replaced in these equations by MT/σ_0^2.

IV. NUMERICAL EVALUATION

The above formulas are meant to provide a simple and rapid means for evaluating P_{fa} for the overlapped FFT processor, and (11)–(13) were coded in FORTRAN using double-precision (64-bit) arithmetic on a VAX computer. As is discussed in more detail below, it was found that the numerical accuracy of the computed results depended on the range of the parameters. Although the summation formula (11) is exact, the numerical results computed with finite-precision arithmetic deteriorate in their accuracy as $\varrho \to 0$. This deterioration results from the large cancellation that occurs between terms of the summation when ϱ approaches zero and the eigenvalues λ_m coalesce to unity. On the other hand, when ϱ is small the fourth-order series approximation in (12) and (13) is suitable for computation, and so the series can be used instead of the summation formula to compute accurate values of P_{fa} for small ϱ.

Several questions therefore need to be answered: for what values of M does the double-precision code give accurate results, and for what values of ϱ should we switch from the summation formula to the series formula? One way of answering these questions, and the approach taken here, is to write supplementary codes that provide an independent check on the results. In this case, two additional codes were written; these codes were written for comparison purposes only, and are not needed in general. The first supplementary code was simply an implementation of formulas (11)–(13) using quadruple- instead of double-precision arithmetic. The results from the quadruple-precision code can be expected to be accurate over a much wider range of parameters than the double-precision code, and can thus be used to pinpoint where the double-precision code starts to become inaccurate. The second supplementary code numerically performed the contour integration of (5); this second code was more complicated (and much slower) than the other codes, but provided a completely independent check. However, numerical instability also led to the necessity of using quadruple-precision arithmetic in the numerical integration when the values of P_{fa} were small ($< 10^{-8}$).

By comparison with the supplementary codes, it was found that the double-precision implementation of formulas (11)–(13) provided accurate values of P_{fa} for $M \leq 16$, with the most accurate results obtained for $M \leq 8$. Such values of M are suitable for the sonar problems that are the author's primary area of interest. Specifically, when $M \leq 8$ the summation formula (11) was used for $\varrho \geq 0.01$, and the series (12) was used for $\varrho < 0.01$. (It is implicit here that the lower and upper bounds for ϱ are 0 and 0.5, respectively.) The computed values of P_{fa} were then found to be accurate for probabilities as small as 10^{-15}, which was the lower limit examined during the comparisons.

As the value of M was increased above 8, the summation formula began to lose accuracy for small values of ϱ, and it became necessary to use the series for a wider range of correlation values. By switching between the series (12) and the summation (11) at $\varrho = 0.05$, the results for P_{fa} were accurate for M as large as 16, but there was reduced accuracy near the switch-over point $\varrho = 0.05$. However, when $\rho > 0.1$ the summation formula (11) will give accurate values of P_{fa} down to at least 10^{-15} over the full range $M \leq 16$. The purpose of the series (12) is to provide values of P_{fa} only for those values $\varrho \approx 0$ where the summation formula fails.

V. SUMMARY AND DISCUSSION

Explicit formulas have been derived for the probability of false alarm of an overlapped FFT processor when the covariance matrix of successive FFT bins is tridiagonal. These formulas are easily coded for the computer and are accurate when the number of overlapped data blocks M is not too large. For large M, the author has found numerical contour integration of (5) to be a good method of evaluation, although more investigation is required to determine the accuracy obtained. The reader will find other techniques of evaluation in [5] and [9]. The formulas given here can also be used to provide an independent check, for moderate values of M, of computer codes based on these more complicated methods of evaluation.

REFERENCES

[1] Whalen, A. D. (1971)
Detection of Signals in Noise.
New York: Academic Press, 1971.

[2] Veeravalli, V. V., and Poor, H. V. (1991)
Quadratic detection of signals with drifting phase.
Journal of the Acoustical Society of America, **89**, 2 (Feb. 1991), 811–819.

[3] Goodman, N. R. (1963)
Statistical analysis based on a certain multivariate complex Gaussian distribution (an introduction).
Annals of Mathematical Statistics, **34** (Mar. 1963), 152–177.

[4] Turin, G. L. (1960)
The characteristic function of Hermitian quadratic forms in complex normal variables.
Biometrika, **47** (1960), 199–201.

[5] Nuttall, A. H. (1970)
Alternate forms for numerical evaluation of cumulative probability distributions directly from characteristic functions.
Proceedings of the IEEE, **58** (1970), 1872–1873.

[6] Proakis, J. G. (1983)
Digital Communications.
New York: McGraw-Hill, 1983, ch. 4.

[7] Jenkins, G. M., and Watts, D. G. (1968)
Spectral Analysis and Its Applications.
Oakland, CA: Holden-Day, 1968, Sect. 2.3.5.

[8] Gradshteyn, I. S., and Ryzhik, I. M. (1980)
Table of Integrals, Series, and Products.
New York: Academic Press, 1980.

[9] Bird, J. S. (1982)
Calculating detection probabilities for systems employing noncoherent integration.
IEEE Transactions on Aerospace and Electronic Systems, **AES-18** (1982), 401–409.

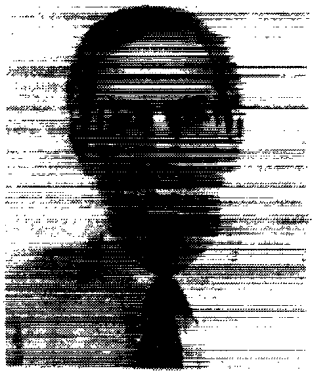

Brian Maranda was born in Vancouver, British Columbia in 1957. In 1979 he received the B.Sc. degree in mathematics and physics, and in 1983 the M.A.Sc. degree in electrical engineering, both from the University of British Columbia.

From 1983 to 1995 he was a member of the Ocean Acoustics Group at the Defence Research Establishment Pacific, where he worked on the application of signal processing to towed-array sonars. In 1995 he joined the Sonar Signal Processing Group at the Defence Research Establishment Atlantic, where he is responsible for the development and performance evaluation of signal-processing algorithms for use in sonar systems. His main interests are in the fields of detection and estimation.

#501385